CHALMERS UNIVERSITY OF TECHNOLOGY | UNIVERSITY OF GOTHENBURG

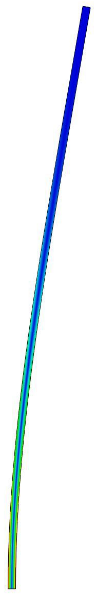

Dynamic Behaviour of a Fixed-end Square Hollow Section Steel Column Subjected to Wind Flow

Engineering Fluid-Structure Interaction (FSI): Technologies and Practices

Final Extensive Project

Ahmad Arafat

Department of Mechanics and Maritime Sciences
CHALMERS UNIVERSITY OF TECHNOLOGY
UNIVERSITY OF GOTHENBURG
Gothenburg, Sweden 2022

Final Extensive Project 2022

Dynamic Behaviour of a Fixed-end Square Hollow Section Steel Column Subjected to Wind Flow

Engineering Fluid-Structure Interaction (FSI): Technologies and Practices

Ahmad Arafat

UNIVERSITY OF GOTHENBURG

CHALMERS
UNIVERSITY OF TECHNOLOGY

Department of Mechanics and Maritime Sciences
Chalmers University of Technology
University of Gothenburg
Gothenburg, Sweden 2022

Dynamic Behaviour of a Fixed-end Square Hollow Section Steel Column Subjected to Wind Flow
Engineering Fluid-Structure Interaction (FSI): Technologies and Practices
Ahmad Arafat

Supervisor: Heng Zhu, Department of Mechanics and Maritime Sciences
Examiner: Hua-Dong Yao, Department of Mechanics and Maritime Sciences

Final Extensive Project 2022
Department of Mechanics and Maritime Sciences
Chalmers University of Technology and University of Gothenburg
SE-412 96 Gothenburg
Telephone +46 31 772 1000

Cover: Von Mises Stress at Time-step 0.0544 s

Typeset in LaTeX
Gothenburg, Sweden 2022

Dynamic Behaviour of a Fixed-end Square Hollow Section Steel Column Subjected to Wind Flow
Ahmad Arafat
Department of Mechanics and Maritime Sciences
Chalmers University of Technology and University of Gothenburg

Abstract

Steel lattice structures are widely used in the structural engineering. These structures are light in weight and usually all structural elements are exposed to wind. This forms that fact that wind loads are highly dependent of the cross-section of structural elements.

Although there are several design codes available for assigning wind loads on lattice structures such as Eurocode - EN 1991-1-4 (2005), the resulted assigned wind loads in these codes are conservative and considering the upper bound solution. Additionally, these codes do not provide clear procedure for investigating the dynamic behaviour of the lattice structures.

Therefore, this project has been directed towards investigating the dynamic behaviour of a fixed-end square hollow section steel column under wind flow. To carry out this project, finite element analysis (FEA) and computational fluid dynamics (CFD) analysis were coupled. The first analysis was built using Abaqus, where the material and boundary conditions of the column were assigned. The second analysis was composed of two steps, where the first step has been aimed to carry out a quasi-steady simulation using STAR-CCM+. Whereas, in the second step, codes of Abaqus and STAR-CCM+ were coupled.

As expected, the column under wind loading will have wind-induced vibration frequencies in both directions (X and Y). The major frequency (in X-direction) is less dependent on mesh size and Time-step. Nevertheless, the minor frequency (in Y-direction) is highly dependent on the mesh size and Time-step, and has lower amplitude.
Finally, calculation according to Eurocode reveals conservative results in comparison with the numerical solutions.

Keywords: Lattice structures, wind flow, fluid-structure interaction (FSI), finite element analysis (FEA), computational fluid dynamics (CFD), Eurocode (EC), Abaqus, STAR-CCM+.

Contents

List of Figures

List of Tables

1
Introduction

1.1 Background

In structural engineering, various materials are used such as concrete, steel and timber. Among all these materials, steel is widely used in structural engineering. Steel has the same capacity in tension and compression, ductile and light in weight. Therefore, the steel structures are considered as light-weight structures. Steel structures have several types such as frame and lattice structures and the latter one can be found in offshore structures, transmission and telecommunication towers and even signboard structures. The common factor between all lattice structures is that all elements are exposed to wind. This results in the fact of that the wind loads on these structures are dependent on the corss-sections of steel. Although there are several design codes available for assigning wind loads on lattice structures such as Eurocode - EN 1991-1-4 (2005) [1], the resulted assigned wind loads in these codes are conservative and considering the upper bound solution [2].

Furthermore, the behaviour of wind is dynamic and in order to assign wind loads, EN 1991-1-4 (2005) simplifies the wind loads to be static loads. This kind of simplification resulted in overestimating the loads and ignoring the dynamic behaviour of the lattice structures.

Therefore, this project has been directed towards investigating the dynamic behaviour of a fixed-end square hollow section steel column under wind flow with a velocity of $40\,m/s$. This column could be part of any lattice structure and its behaviour can give an indication on how slender structural elements could behave in a lattice structure.

1.2 Aim

The main outcome of this project was to enrich knowledge about the behaviour of lattice structures under wind loading by:

- Studying the dynamic structural behaviour of the studied column under wind loading.
- Investigating any discrepancy between analytical and numerical solutions.

1.3 Limitations

The project aimed to investigate various aspects, which are related to the project's topic , but there were several limitations precluded studying the following factors:

- Effect of Rayleigh Damping factors, which are α and β.
- Assessing the dynamic structural behaviour under different wind velocities.

2

Methods

In order to carry out this project, it has been broken down into three phases. These phases are illustrated in the following sections:

2.1 Finite Element Analysis (FEA) using Abaqus

The studied column in this project is a square hollow section steel column. This column is fixed in one end, where the other end is free. The length of the column is $1.5\,m$ and its section is depicted in Figure **2.1**.

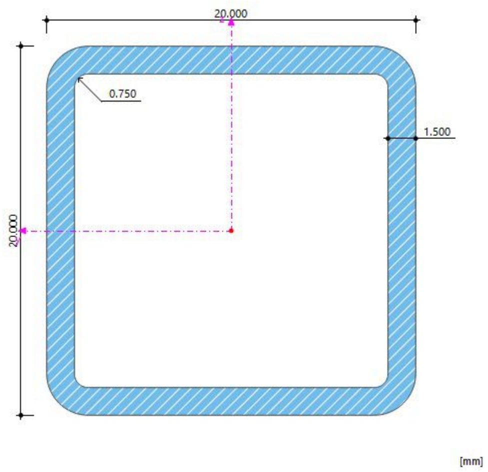

Figure 2.1: Square Hollow Section

In order to perform a FEA using Abaqus that can be coupled later to STAR-CCM+, firstly, a sketch of the studied section has been drawn and then extruded. The studied material is steel (S235J2) and its properties are illustrated in Table **2.1**. It is worth to mention that the β value has been chosen arbitrarily based on the third exercise in this course. The section in Abaqus has been chosen to be Solid and Homogeneous. To mesh the part, the mesh type has been set to be linear hexahedral (C3D8R) and the resulted number of nodes and elements were 5270 and 2820, respectively (see Figure **2.2**).

Table 2.1: Properties of Steel (S235J2)

S235J2	Unit	Values
Density	$[kg/m^3]$	7850
Poisson's ratio	$[-]$	0.3
Young's modulus	$[GPa]$	200
Damping factor (β)	$[-]$	$10^{-}6$

The next step of creating the finite element model was to assign steps and boundary conditions. Two steps were assigned, where the first one is Initial and the second one is Dynamic Implicit. The details of the Dynamic Implicit step such as maximum increment size and maximum number of iterations can be found in Appendix **A**. For the boundary conditions, one end (lower surface) has been chosen to be fixed (ENCASTRE), where the other end is free. Additionally, the surfaces (Upper, Inner and Outer) that are expected to be subjected to wind pressure have been defined (see Appendix **A**).

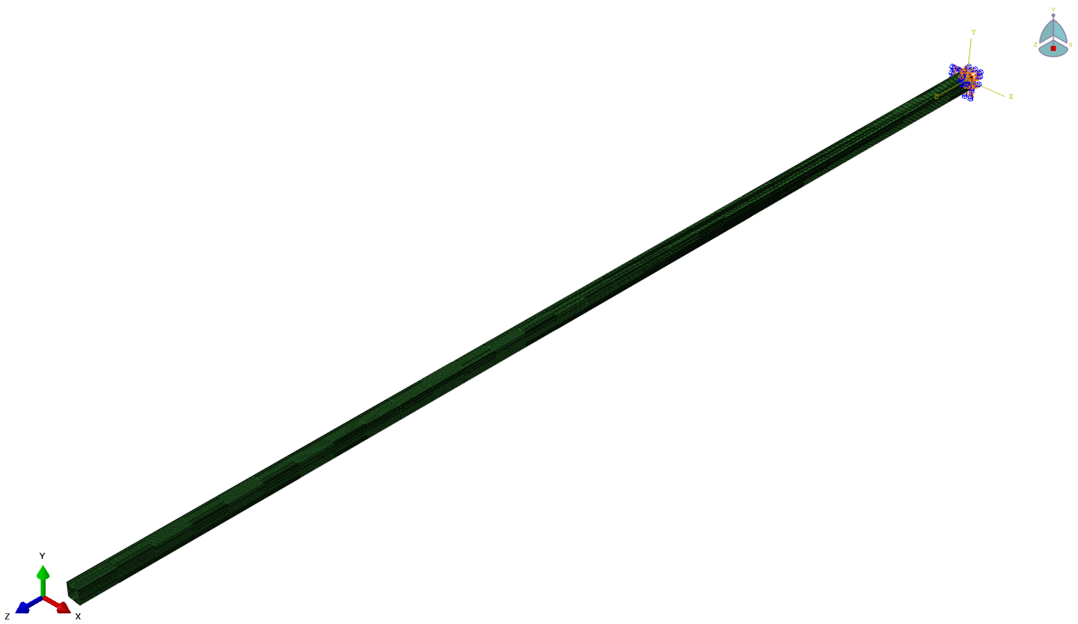

Figure 2.2: Mesh and Boundary Conditions - Abaqus

2.2 Computational Fluid Dynamic (CFD) Simulation using Simcenter STAR-CCM+

The aim of CFD simulation was to perform a quasi-steady simulation, which can be used later as the initial condition for the co-simulation. To carry out the quasi-steady simulation, the first step was to import the built geometry of the column from Abaqus. The second step was to create the geometry of air domain, where the size of the domain and the location of the column are shown in Figure **2.3**. Thence, both geometries have been split by patch and subtracted.

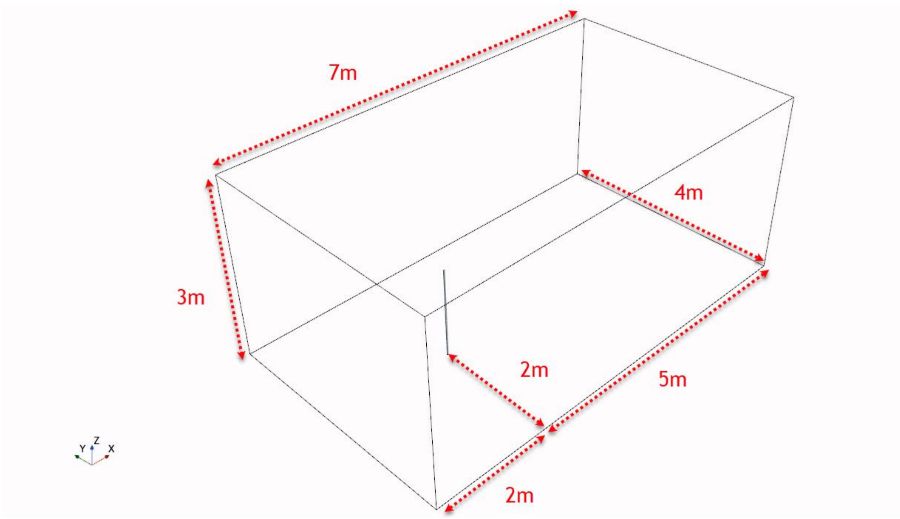

Figure 2.3: Air Domain Size

In order to mesh the domain, the following meshers have been chosen:

- Surface Remesher
- Polyhedral Mesher
- Prisim Layer Mesher

Furthermore, the mesh has been refined by surface control, which resulted in finer mesh around the column. Two mesh sizes (see Tables **2.2** and **2.3**) have been considered in this project in order to perform mesh sensitivity analysis.

Table 2.2: Mesh 1 Controls

Controls	Unit	Domain	Surface
Max/Min cell size	$[m]$	0.05/0.01	0.05/0.001
Number of prisim layers	$[-]$	5	15
Prisim layer thotal thickness	$[m]$	0.05	0.001
Maximum skewness angle	$[deg]$	84.8	
Total number of cells	$[-]$	580163	

Table 2.3: Mesh 2 Controls

Controls	Unit	Domain	Surface
Max/Min cell size	$[m]$	0.05/0.0005	0.05/0.0005
Number of prisim layers	$[-]$	5	15
Prisim layer thotal thickness	$[m]$	0.005	0.005
Maximum skewness angle	$[deg]$	84.6	
Total number of cells	$[-]$	1560732	

For this simulation, one physics continuum for air were required, where the assigned models can be seen in Table **2.4**.

Table 2.4: Models for Air Continuum

Group	Model
Enabled Models	Three-Dimensional
Time	Implicit Unsteady
Material	Gas
Flow	Segregated Flow
	Gradients
Equation of State	Constant Density
Viscous Regime	Turbulent
	Reynolds-Averaged Navier-Stokes
Reynolds-Averaged Turbulence	K-Epsilon Turbulence
	Realizable K-Epsilon Two-Layer
	Two-Layer All y+ Wall Treatment
Optional Models	Cell Quality Remediation
	Solution Interpolation

The next step in this phase was to set up the initial velocity and turbulence intensity, and define the boundary conditions. Since this project is directed towards structural engineering, the turbulence intensity were calculated according Eurocode - EN 1991-1-4 (2005) [1] (see Appendix **B**). For the initial conditions the turbulence intensity and the initial velocity has been set to be 0.161 and $40\,m/s$, respectively, where the flow direction is in X-direction.

Thenceforward, the boundary conditions have been assigned as illustrated in Figure **2.4**. The type of inlet has been chosen to be Velocity Inlet with the same initial conditions and the outlet type was Pressure Outlet.

Lastly in this phase, the Time-Step has been set to be $1.5\,s$ and the Temporal Discretization was first-order. One stopping criterion has been assigned, which is the Maximum Inner Iteration and it was limited to 400 steps.

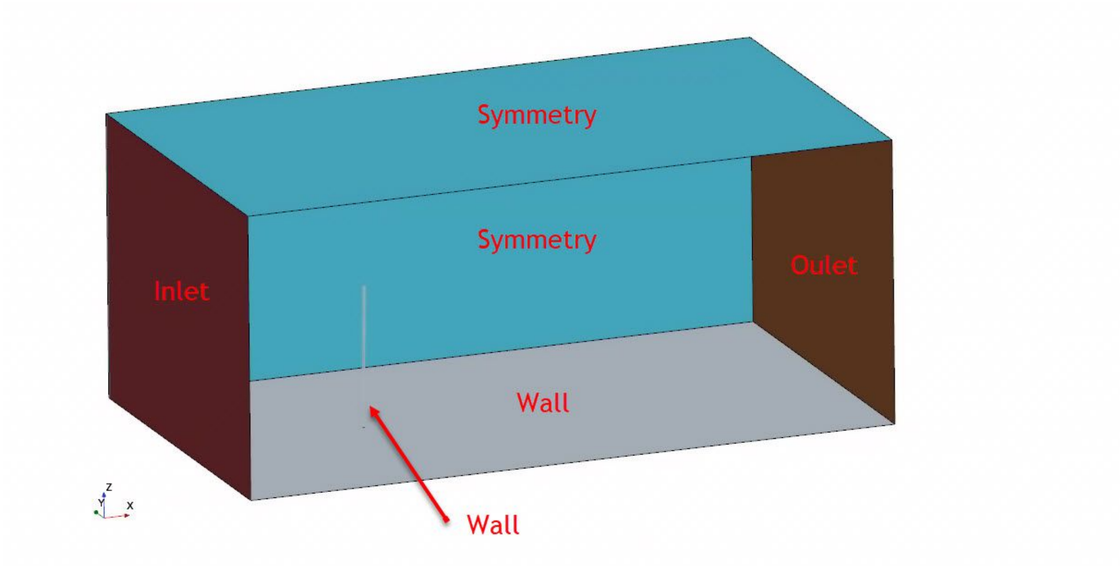

Figure 2.4: Boundary Conditions for CFD Simulation

2.3 Co-simulation Using Simcenter STAR-CCM+ and Abaqus

In this phase, both codes (Simcenter STAR-CCM+ and Abaqus) were coupled, where data is exchanging between codes. Simcenter STAR-CCM+ passes traction loads to Abaqus (pressure + wall shear stress), and Abaqus passes displacements to Simcenter STAR-CCM+. The first step of this phase was to adjust the air continuum and define another continuum for solid. In the continuum of air, new optional models have been added (see Table **2.5**). For the continuum of solid, Simcenter STAR-CCM+ were connected to Abaqus and the chosen models are shown in Table **2.6**.

Table 2.5: Optional Models for Air Continuum

Group	Model
Optional Models	Co-Simulation
Co-Simulation Models	Abaqus
Abaqus Coupling Models	Abaqus Explicit Coupling

Table 2.6: Models for External Solid Continuum

Group	Model
Optional Models	External Continuum
External Continuum	External Application
External Application	Abaqus
Time	Implicit Unsteady
Optional Models	Surface Three Dimensional

Next step was to set deformation of mesh due to displacement of the column. This has been achieved by assigning Morphing Motion to fluid surfaces of the column. Whereas, the inlet and outlet boundaries were constrained for mesh movement. Moreover, Automatic Thin-out Cl factor has been used and set to be 0.5. Besides, the morph settings were changed to Morph from Zero to to prevent inaccuracies from accumulating during the simulation. As a penultimate step, a reference point has been created to measure the displacement, where this point is facing the wind direction and it is in the middle of the outer column's edge. Ultimately, two different time-steps have been considered for the solver of implicit unsteady, one is $0.004\,s$ and the other is $0.00068\,s$. Besides, the Temporal Discretization has been changed to second-order. In addition, the Maximum Inner Iterations has been set to be 10 and different Maximum Physical Time were studied.

3

Results

In this chapter, results of different simulations are presented in the following sections:

3.1 Mesh 1, Maximum Physical Time ($2\,s$), Time-step ($0.004\,s$)

In order to get an overview of how the column will behave under wind loading, firstly, a coarse mesh (see Table **2.2** and Figure **3.1**) has been used. Additionally, the considered Maximum Physical Time and Time-step were $2\,s$ and $0.004\,s$, respectively.

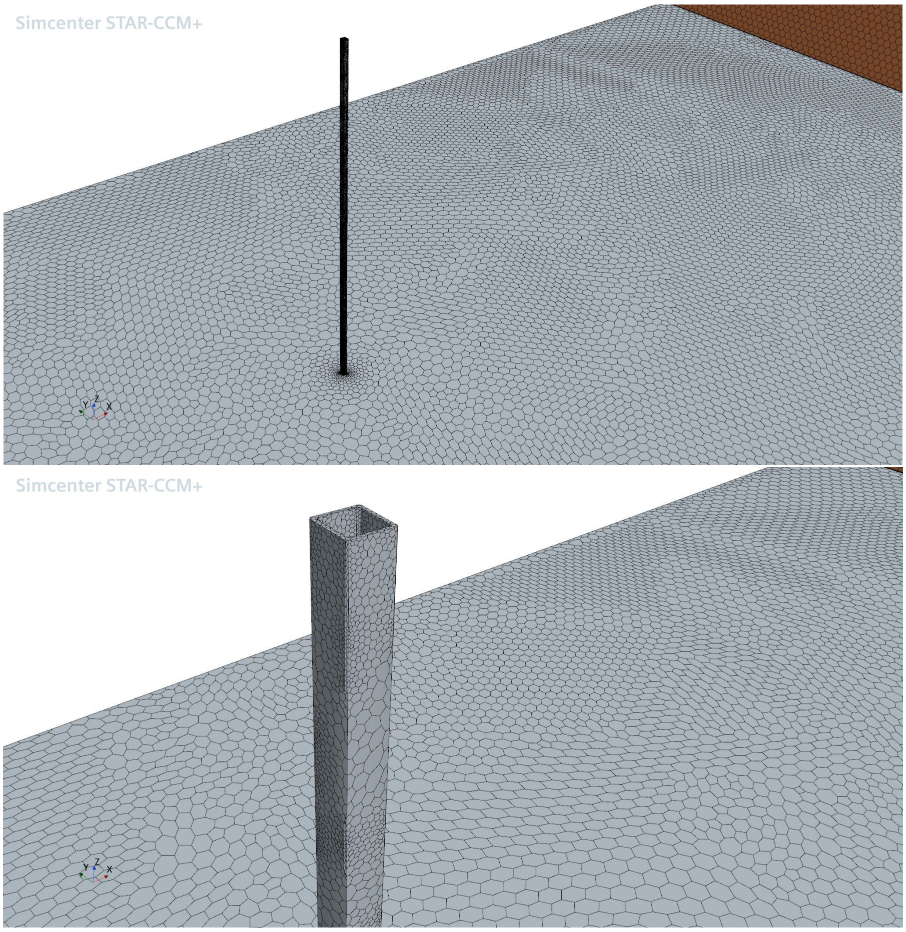

Figure 3.1: Mesh 1 - STAR-CCM+

This simulation resulted in the following displacements in X- and Y-direction (see Figures **3.2** and **3.3**). This implies that the column has wind-induced vibration frequencies in both directions. Additionally, Figure **3.2** revealed that the first bending mode in X-direction occurred at time $0.052\,s$ with maximum displacement of $19.7\,mm$ and the frequency was $9.6\,Hertz$. Whereas, Figure **3.3** exhibited that the first bending mode in Y-direction occurred at the same time $0.052\,s$, but with maximum displacement of $0.67\,mm$.

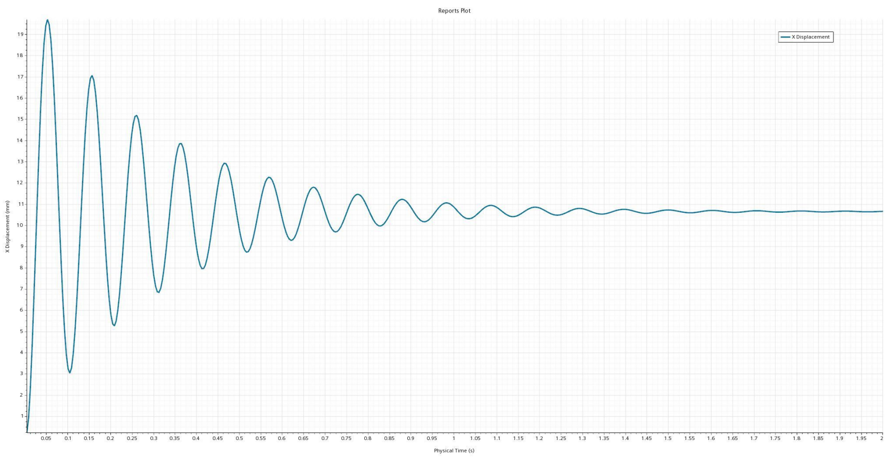

Figure 3.2: Displacement in X-direction - Simulation 1

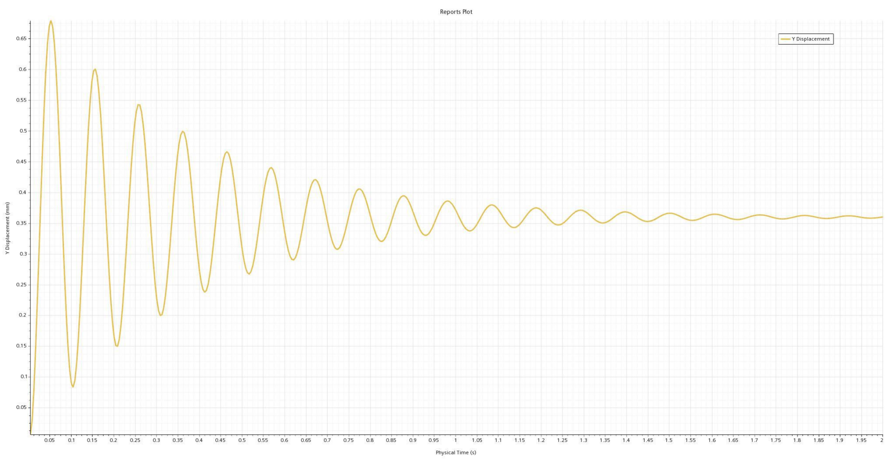

Figure 3.3: Displacement in Y-direction - Simulation 1

Moreover, the acting forces (pressure and shear) and moment can be seen in the following Figures **3.4** and **3.5**, where the maximum force and moment were $36.1\,N$ and $2.8\,N.mm$, respectively.

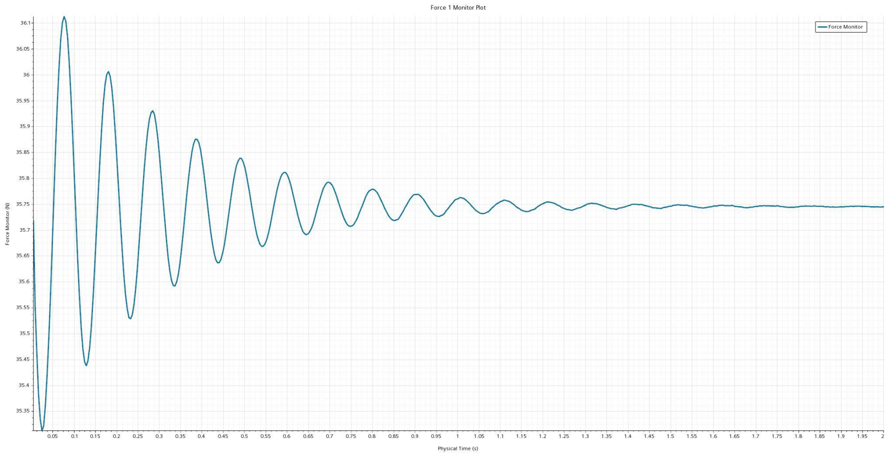

Figure 3.4: Force Plot - Simulation 1

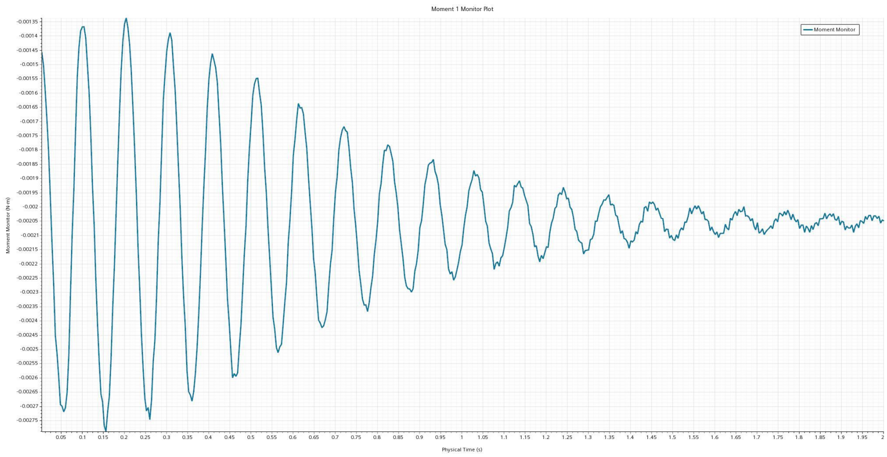

Figure 3.5: Moment Plot - Simulation 1

3.2 Mesh 2, Maximum Physical Time ($2\,s$), Timestep ($0.004\,s$)

In order to capture more exact dynamic behaviour of the column, a refined mesh (see Table **2.3** and Figure **3.6**) has been used.

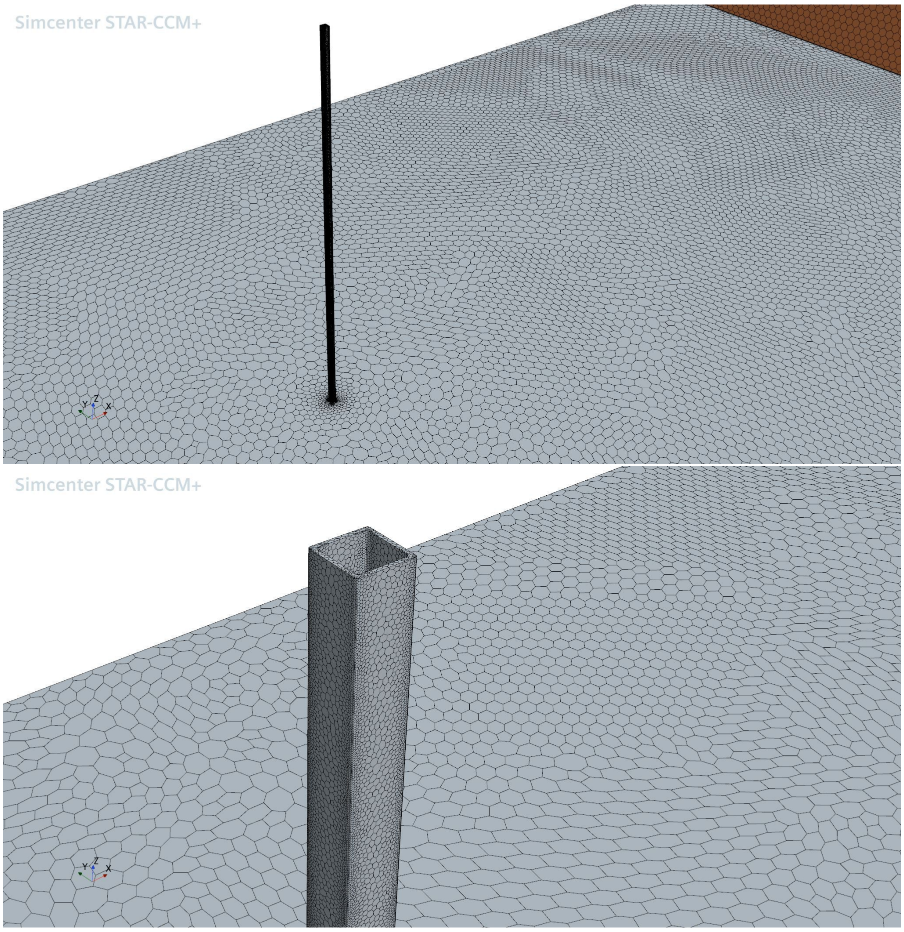

Figure 3.6: Mesh 2 - STAR-CCM+

The second simulation resulted in the following displacements in X- and Y-direction (see Figures **3.7** and **3.8**). Furthermore, Figure **3.7** revealed that the first bending mode in X-direction occurred at time $0.052\,s$ with maximum displacement of $18.04\,mm$ and the frequency was $9.6\,Hertz$. Whereas, Figure **3.8** exhibited that the first bending mode in Y-direction occurred at time $0.02\,s$, but with maximum displacement of $1.18\,mm$.

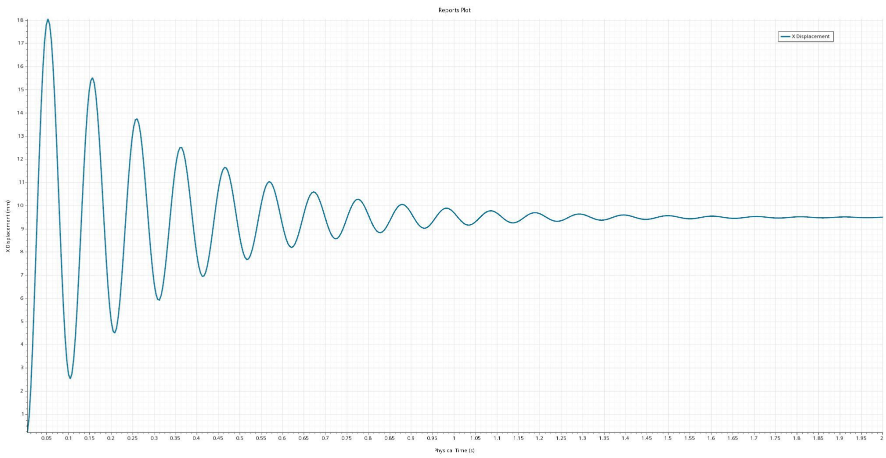

Figure 3.7: Displacement in X-direction - Simulation 2

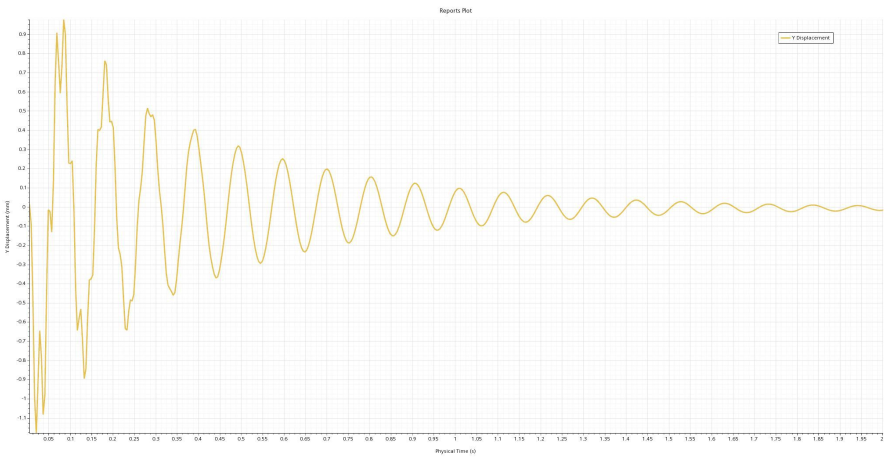

Figure 3.8: Displacement in Y-direction - Simulation 2

Moreover, the acting forces (pressure and shear) and moment can be seen in the following Figures **3.9** and **3.10**, where the maximum force and moment were 32.65 N and 98.9 $N.mm$, respectively.

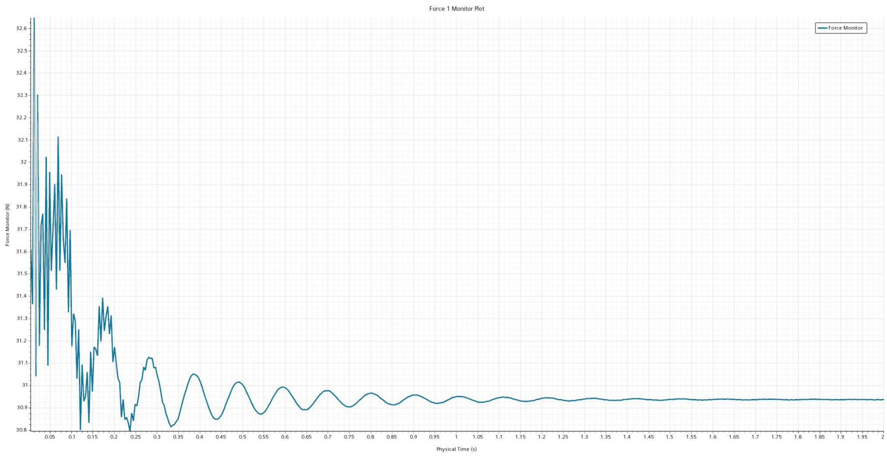

Figure 3.9: Force Plot - Simulation 2

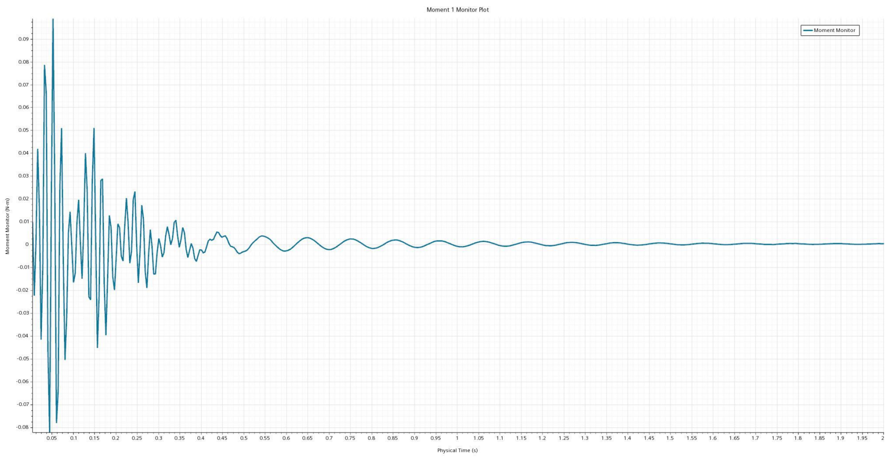

Figure 3.10: Moment Plot - Simulation 2

3.3 Mesh 2, Maximum Physical Time ($0.34\,s$), Time-step ($0.00068\,s$)

The aim of this simulation is to capture the first three bending modes more accurately with the mesh controls 2 (see Table **2.3**). Therefore, the Maximum Physical Time and Time-Step have been reduced to be $0.34\,s$ and $0.00068\,s$, respectively. The third simulation resulted in the following displacements in X- and Y-direction (see Figures **3.11** and **3.12**). Furthermore, Figure **3.11** revealed that the first bending mode in X-direction occurred at time $0.051\,s$ with maximum displacement of $19.51\,mm$ and the frequency was $9.7\,Hertz$. Whereas, Figure **3.12** exhibited that the first bending mode in Y-direction occurred at time $0.029\,s$, but with maximum displacement of $0.43\,mm$, respectively.

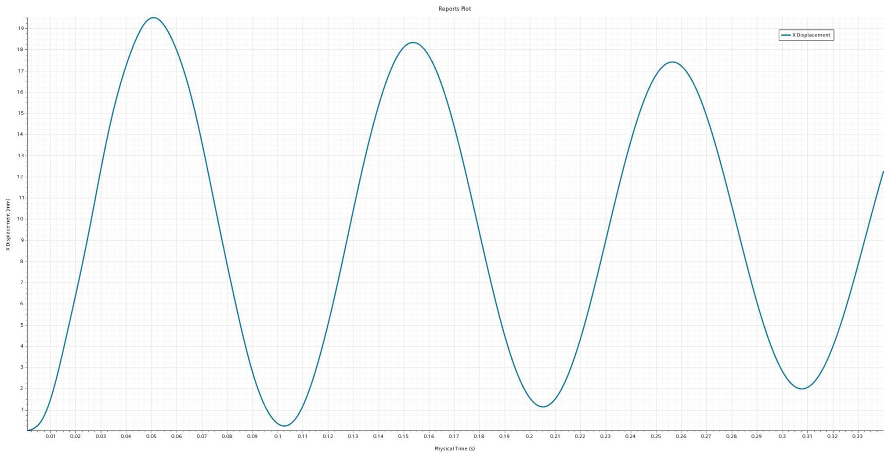

Figure 3.11: Displacement in X-direction - Simulation 3

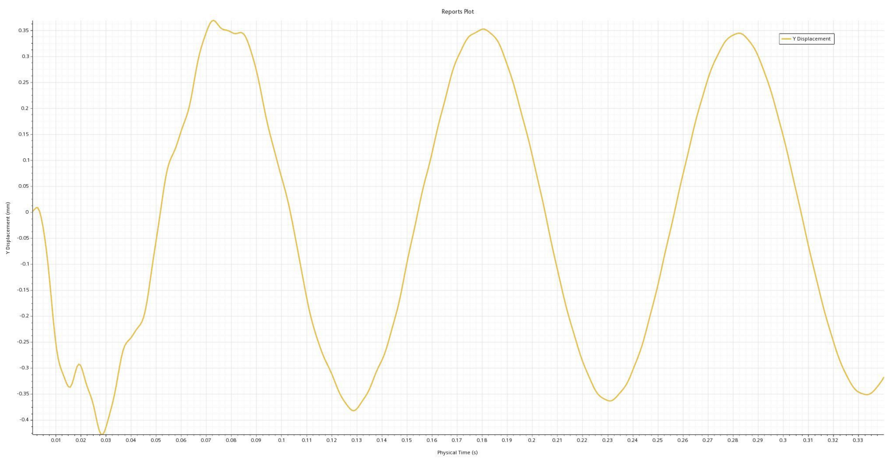

Figure 3.12: Displacement in Y-direction - Simulation 3

Moreover, the acting forces (pressure and shear) and moment can be seen in the following Figures **3.13** and **3.14**, where the maximum force and moment were $34.28\,N$ and $44.3\,N.mm$.

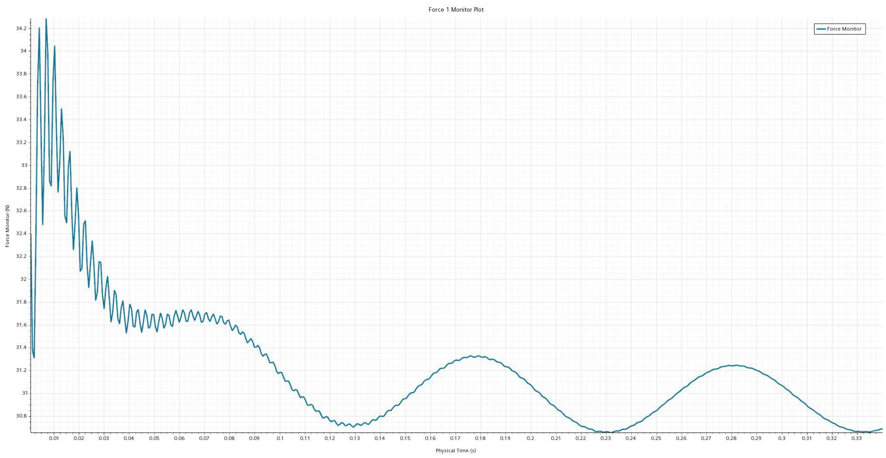

Figure 3.13: Force Plot - Simulation 3

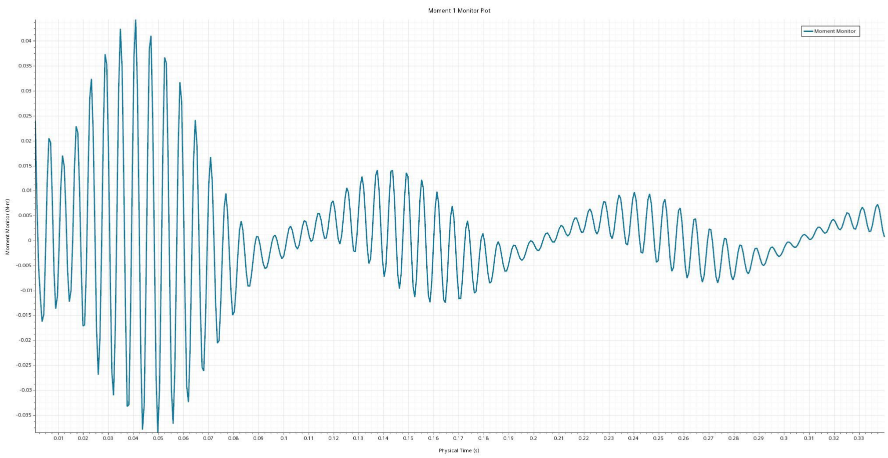

Figure 3.14: Moment Plot - Simulation 3

For this simulation, the results of pressure and velocity for the first bending mode in X-direction are presented in Figures **3.15** and **3.16**. In addition, Figure **3.17** depicted how morpher deformed the mesh throughout the air region.

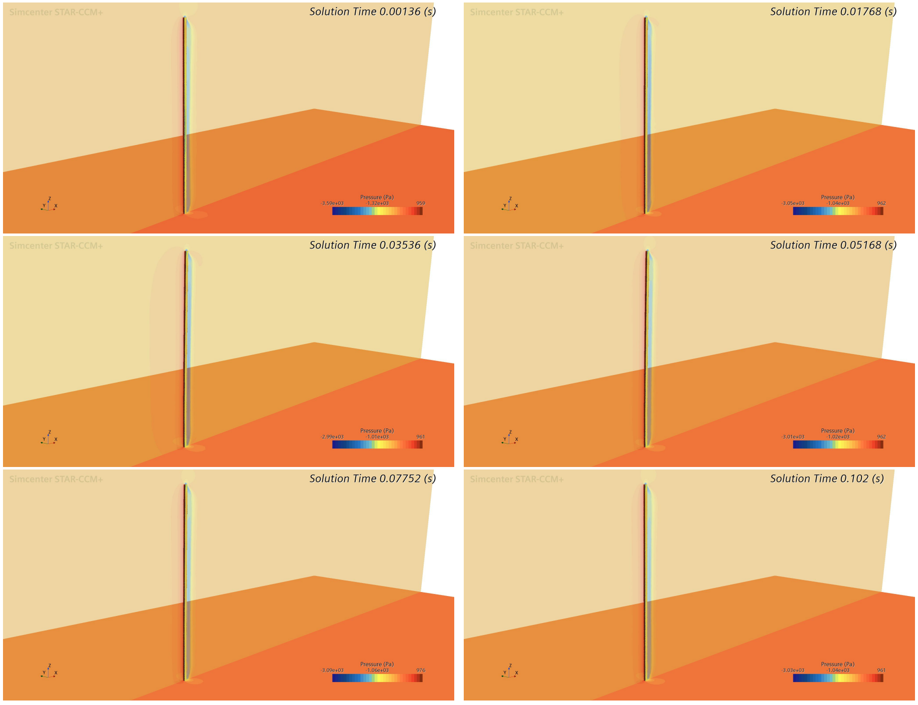

Figure 3.15: Pressure Scene - Simulation 3

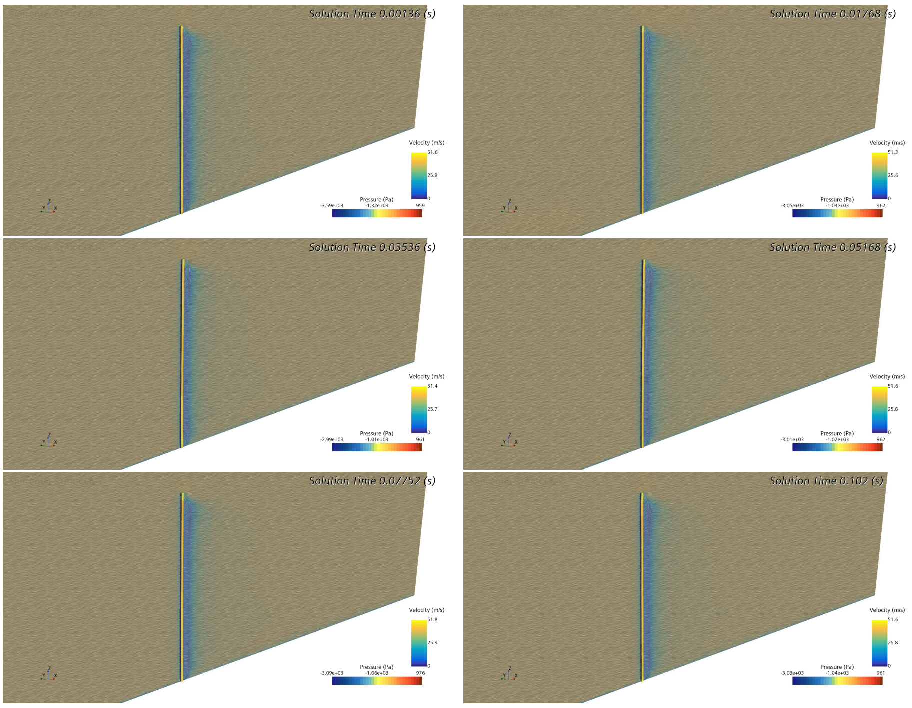

Figure 3.16: Velocity Scene - Simulation 3

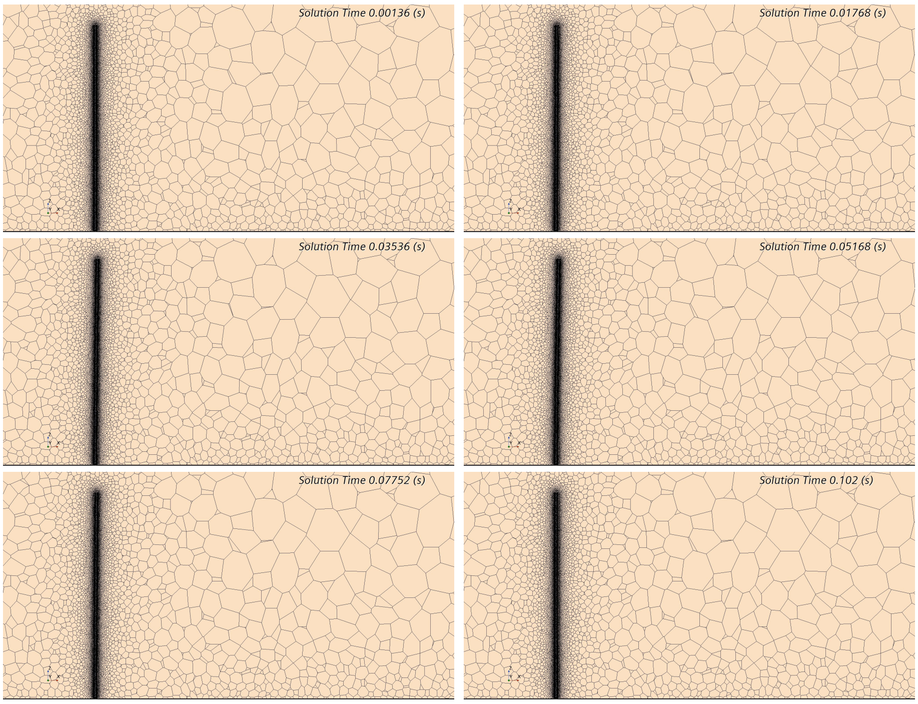

Figure 3.17: Mesh Morphing Scene - Simulation 3

Finally, Figures **3.18** and **3.19** exhibited Von Mises stress and deflection at time $0.0544\,s$, where maximum Von Mises stress was $61.95\,N/mm^2$ and maximum deflection was $19.23\,mm$.

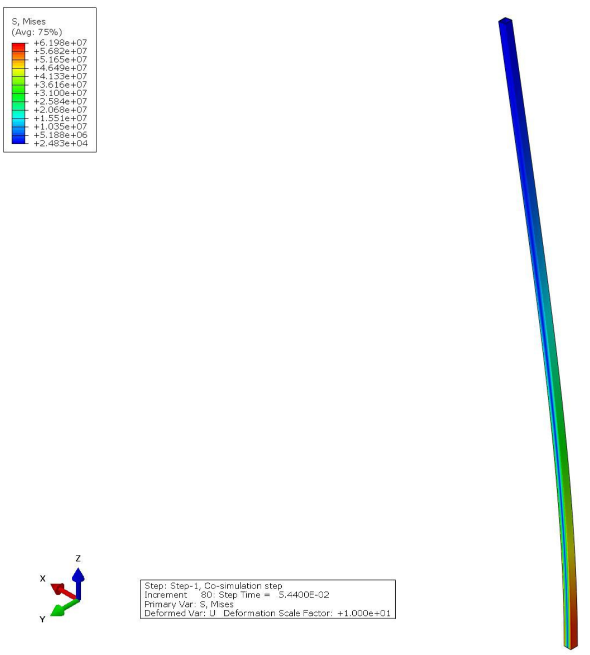

Figure 3.18: Von Mises Stress - Simulation 3

Figure 3.19: Displacement - Simulation 3

4

Discussion and Conclusion

All results demonstrated that the column under wind loading will have wind-induced vibration frequencies in both directions X and Y. Additionally, results revealed that the frequent movement will stagnate and reach low frequency after $2\,s$. This implies that the mesh size in this project did not play a significant role in predicting the overall dynamic behaviour. Moreover, the displacement in X-direction, in all three simulations, exhibited similar results, where the maximum displacement varied between $18.04\,mm$ and $19.7\,mm$ (Maximum difference 8.4%). Whereas, the frequency in X-direction did not show a remarkable change.

On the other hand, results revealed that the behaviour of the column in Y-direction is more complicated, where the three simulations revealed different results. For instance, the first simulation (see Section **3.1** and Figure **3.3**) exhibited that the displacement fluctuated solely in the positive Y-direction and stagnated with keeping a positive displacement. In other words, the column, after damping, had low frequent behaviour in the positive Y-direction. This behaviour is illogical since the column has a homogeneous material (steel) and a symmetric cross-section, and the air flow around the column shall be symmetric as well. Anyhow, this behaviour could spring from the inability of the mesh in STAR-CCM+ to form a symmetric cross-section, which could result in asymmetric load distribution in Abaqus.

On the contrary, the second simulation (see Section **3.2** and Figure **3.8**) revealed more logical behaviour in Y-direction, where after damping, the amplitude was around zero. This implies that the column, first, will have remarkable amplitude in the positive and negative Y-direction and then keeps a low amplitude around zero.

The third simulation (see Section **3.3** and Figure **3.12**) demonstrated a better overview of how the column behaved in Y-direction. Besides, the maximum displacement in Y-direction was less, where the difference between the second simulation and third one was 63.55%.

Regarding the acting force, all three simulations (see Figures **3.4**, **3.9** and **3.13**) showed similar maximum force, where the maximum force varied between $36.1\,kN$ and $34.28\,kN$ (Maximum difference 5%). Nevertheless, the acting moment (see Figures **3.5**, **3.10** and **3.14**) showed a huge difference between all three simulations. The first simulation showed out of range maximum moment, and the moment dropped 55.2% from the second simulation to the third simulation. This implies that the acting moment was sensitive to both the mesh size and Time-Step.

Furthermore, the wind action on this column has been calculated according to Eurocode (see Appendix **B**) in order to investigate any discrepancy between the numerical solution (third simulation) and analytical solution (Eurocode calculation). The results of Eurocode calculation demonstrated that the maximum deflection and Von Mises stress are $27.7\,mm$ (Figure **B.6**) and $101.58\,N/mm^2$ (Figure **B.7**), respectively. This implies that there is a difference of almost 39% between the analytical and numerical solutions. This could be attributed to the upper bond solution that Eurocode considers.

As a conclusion, the dynamic behaviour of the column under wind loading is composed of two wind-induced vibration frequencies in two directions. The main frequency (in X-Direction) showed small dependency on the mesh size and Time-Step, whereas the minor frequency (in Y-direction) was highly dependent on the mesh size and Time-Step, and had lower amplitude in comparison with the main one. Moreover, the maximum acting force of the column was similar in all simulations, but the maximum acting moment was different in all simulation and showed high dependency on the mesh size and Time-Step. Ultimately, the wind calculation according to Eurocode was conservative and resulted in overestimation of the maximum deflection and Von Mises Stress.

Bibliography

[1] EN 1991-1-4 (2005). Eurocode 1: Actions on structures - Part 1-4: General actions - Wind actions

[2] COSTA, A., PAIVA, F. and BARROS, R., 2014, December. Aerodynamic Study of Wind Flow through a Lattice Tower of Angular Section Profiles, Using Computational Fluid Dynamics. In 2014 International Conference on Mechanics and Civil Engineering (icmce-14) (pp. 83-87). Atlantis Press.

A

Input File for Abaqus

The aim of appending the input Abaqus file is to show several things such as material properties, boundary conditions as well as coupling commands. Therefore, several sections have been truncated.

```
*Heading
** Job name: ProjectJob_A03 Model name: Project_Model
** Generated by: Abaqus/CAE 2020.HF3
*Preprint, echo=NO, model=NO, history=NO, contact=NO
**
** PARTS
**
*Part, name=Project_Geo
*Node
      1, -0.00978032965, 0.00978032965,          1.5
      2, -0.00925000012, 0.00999999978,          1.5
      3, -0.00999999978, 0.00925000012,          1.5
      .
      .
      Truncated
      .
      .
*Element, type=C3D8R
   1,    1,  154,  157,    3,  171,  324,  327,  173
   2,  161,  124,   16,  160,  331,  294,  186,  330
      .
      .
      Truncated
      .
      .
*Elset, elset=_FSI_INTERFACE_S4, internal, instance=Project_Geo-1
    2,    5,    7,    .. Truncated ..   28,   34
   36,   37,   38,    .. Truncated ..   67,   70
      .
      .
      Truncated
      .
```

```
      .
*Elset, elset=_FSI_INTERFACE_S5, internal, instance=Project_Geo-1
    4,    9,   11,    .. Truncated ..   41,   42
   43,   44,   45,    .. Truncated ..   79,   80
      .
      .
      Truncated
      .
      .
*Elset, elset=_FSI_INTERFACE_S1, internal, instance=Project_Geo-1,
 generate
  1,  94,   1
*Surface, type=ELEMENT, name=FSI_INTERFACE
_FSI_INTERFACE_S6, S6
_FSI_INTERFACE_S4, S4
_FSI_INTERFACE_S3, S3
_FSI_INTERFACE_S5, S5
_FSI_INTERFACE_S1, S1
*End Assembly
**
** MATERIALS
**
*Material, name=STEEL
*Damping, beta=1e-06
*Density
7850.,
*Elastic
 2.1073e+11, 0.3
*Plastic
 2.002e+08,     0.
  2.46e+08, 0.0235
  2.94e+08, 0.0474
  3.74e+08, 0.0935
  4.37e+08, 0.1377
   4.8e+08,   0.18
**
** INTERACTION PROPERTIES
**
*Surface Interaction, name=IntProp-1
1.,
*Friction
0.,
*Surface Behavior, pressure-overclosure=HARD
**
** BOUNDARY CONDITIONS
**
```

```
** Name: Disp-BC-1 Type: Symmetry/Antisymmetry/Encastre
*Boundary
SET-1, ENCASTRE
**
** INTERACTIONS
**
** Interaction: GeneralContact
*Contact
*Contact Inclusions, ALL EXTERIOR
*Contact Property Assignment
 ,  , IntProp-1
** ----------------------------------------------------------------
**
** STEP: Step-1
**
*Step, name=Step-1, nlgeom=YES, inc=1000000
Co-simulation step
*Dynamic,alpha=-0.05,haftol=100000.
0.00068,2.,6e-05,0.00068
**
** OUTPUT REQUESTS
**
*Restart, write, frequency=0
**
** FIELD OUTPUT: F-Output-1
**
*Output, field, variable=PRESELECT
**
** HISTORY OUTPUT: H-Output-1
**
*Output, history, variable=PRESELECT
**
*CO-SIMULATION, NAME=Project, PROGRAM=MULTIPHYSICS,
CONTROLS=Control
*CO-SIMULATION REGION, TYPE=SURFACE, EXPORT
ASSEMBLY_FSI_INTERFACE, U
*CO-SIMULATION REGION, TYPE=SURFACE, IMPORT
ASSEMBLY_FSI_INTERFACE, CF
*CO-SIMULATION CONTROLS, NAME=Control,
COUPLING SCHEME=GAUSS-SEIDEL, SCHEME MODIFIER=LEAD,
STEP SIZE=6.8E-4, TIME INCREMENTATION=SUBCYCLE,
TIME MARKS=YES
**
*End Step
```

B

Calculation according to Eurocode

B.1 Wind Velocity and Velocity Pressure

As a first step, the chosen basic wind velocity (v_b) for this project is $40\,m/s$ and the height of the column (z) is $1.5\,m$.

B.1.1 Definition of Terrain Category and Terrain Parameters

It has been assumed in this project that the studied column is located in a coastal area; hence according to Figure **B.1**, the terrain category is 0. Based on the specified terrain category, the roughness length (z_0) and minimum height (z_{min}) are $0.003\,m$ and $1\,m$, respectively. Additionally, the terrain orography ($c_0(z)$) has been assumed to be 1, where EN 1991-1-4 (2005) [1] states that the effects of orography may be neglected when the average slope of the upwind terrain is less than 3°.

	Terrain category	z_0 m	z_{min} m
0	Sea or coastal area exposed to the open sea	0,003	1
I	Lakes or flat and horizontal area with negligible vegetation and without obstacles	0,01	1
II	Area with low vegetation such as grass and isolated obstacles (trees, buildings) with separations of at least 20 obstacle heights	0,05	2
III	Area with regular cover of vegetation or buildings or with isolated obstacles with separations of maximum 20 obstacle heights (such as villages, suburban terrain, permanent forest)	0,3	5
IV	Area in which at least 15 % of the surface is covered with buildings and their average height exceeds 15 m	1,0	10
NOTE: The terrain categories are illustrated in A.1.			

Figure B.1: Terrain Categories and Terrain Parameters

B.1.2 Calculation of Turbulence Intensity

The recommended value of the turbulence factor (k_1) in EN 1991-1-4 (2005) [1] is 1. Thus, the turbulence intensity can be calculated according to the following equation:

$$I_v(z) = \begin{cases} \frac{k_1}{c_0(z) \cdot \ln(z/z_0)} & z_{min} \leq z \leq z_{max} \\ I_v(z_{min}) & z < z_{min} \end{cases} \tag{B.1}$$

The application of Equation **B.1** results in a turbulence intensity of 0.161.

B.1.3 Calculation of Roughness Factor (c_r)

This factor can be calculated according to Equation **B.2**.

$$c_r(z) = \begin{cases} k_r \cdot \ln(z/z_0) & z_{min} \leq z \leq z_{max} \\ c_r(z_{min}) & z < z_{min} \end{cases} \tag{B.2}$$

The application of Equation **B.2** results in a value of 0.970.

B.1.4 Calculation of Mean Wind Velocity (v_m)

The mean wind velocity can be determined by using the following expression:

$$v_m(z) = c_r(z) \cdot c_0(z) \cdot v_b \tag{B.3}$$

The application of Expression **B.3** results in a mean wind velocity of 38.788 m/s.

B.1.5 Calculation of Peak Velocity Pressure (q_p)

The peak velocity pressure can be calculated according to the following equation:

$$q_p(z) = [1 + 7 \cdot I_v(z)] \cdot 0.5 \cdot \rho \cdot (v_m)^2(z) \tag{B.4}$$

The application of Equation **B.4** results in a peak velocity pressure of 1.4 kN/m^2.

B.2 Force Coefficient of Square Section with Rounded Corners

In order to calculate the force coefficient for the studied cross-section, first, the force coefficient of rectangular sections with sharp corners and without free-end flow ($c_{f,0}$) shall be calculated according to the Figure **B.2**, which results in a coefficient of 2.1.

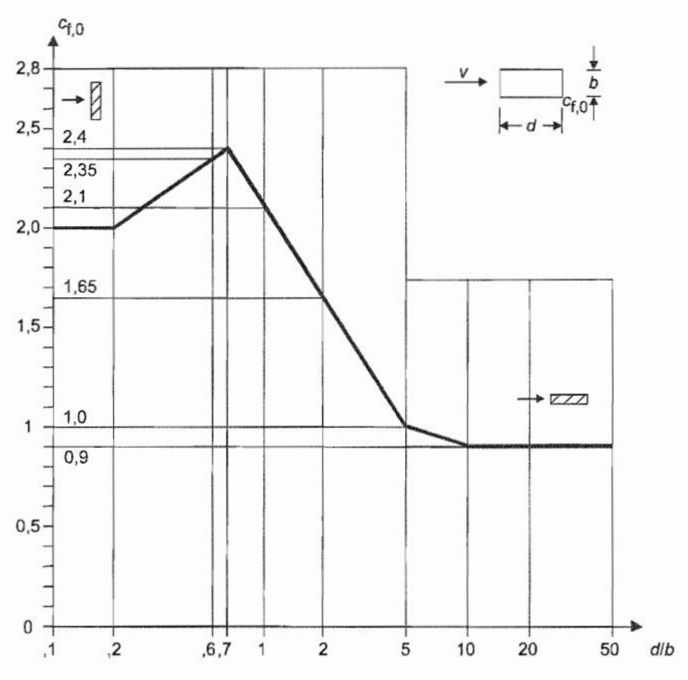

Figure B.2: Force Coefficients $c_{f,0}$ of Rectangular Sections with Sharp Corners and Without Free End Flow

Thence, the reduction factor for square sections with rounded corners (ψ_r) can be calculated according to the Figure **B.3**, which results in a value of 1.

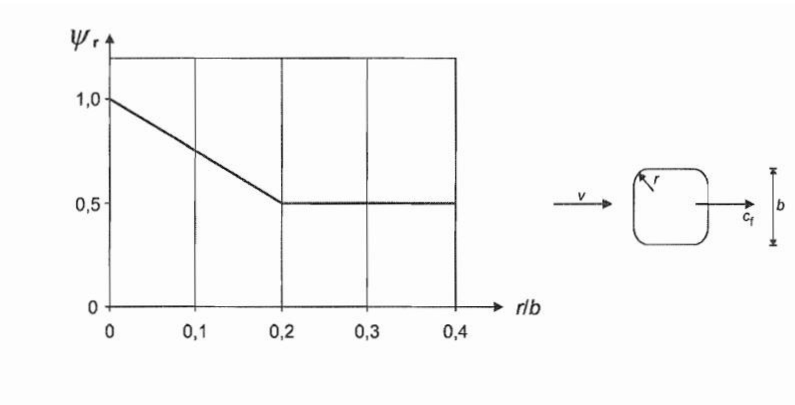

Figure B.3: Reduction Factor ψ_r for a Square Cross-section with Rounded Corners

As a penultimate step, the end-effect factor (ψ_λ) can be calculated according to Figures **B.4** and **B.5** , where the solidity ratio (φ) is 1.

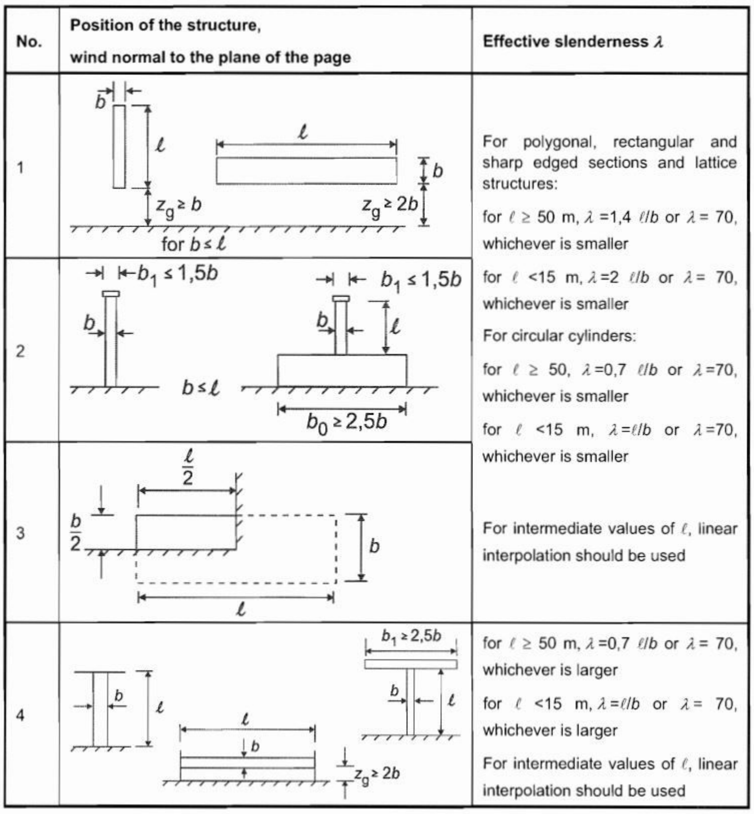

No.	Position of the structure, wind normal to the plane of the page	Effective slenderness λ
1		For polygonal, rectangular and sharp edged sections and lattice structures: for $\ell \geq 50$ m, $\lambda = 1{,}4\ \ell/b$ or $\lambda = 70$, whichever is smaller
2		for $\ell < 15$ m, $\lambda = 2\ \ell/b$ or $\lambda = 70$, whichever is smaller. For circular cylinders: for $\ell \geq 50$, $\lambda = 0{,}7\ \ell/b$ or $\lambda = 70$, whichever is smaller; for $\ell < 15$ m, $\lambda = \ell/b$ or $\lambda = 70$, whichever is smaller
3		For intermediate values of ℓ, linear interpolation should be used
4		for $\ell \geq 50$ m, $\lambda = 0{,}7\ \ell/b$ or $\lambda = 70$, whichever is larger; for $\ell < 15$ m, $\lambda = \ell/b$ or $\lambda = 70$, whichever is larger; For intermediate values of ℓ, linear interpolation should be used

Figure B.4: Recommended Values of λ for Cylinders, Polygonal Sections, Rectangular Sections, Sharp Edged Structural Sections and Lattice Structures

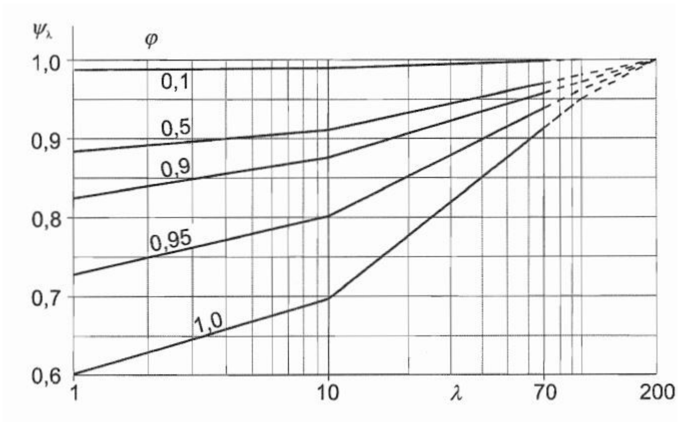

Figure B.5: Indicative Values of the End-effect Factor ψ_λ as a Function of Solidity Ratio φ Versus Slenderness λ

Hence, the force coefficient (c_f) of the studied column can be determined by using the following expression:

$$c_f = c_{f,0} \cdot \psi_r \cdot \psi_\lambda \tag{B.5}$$

Which results in a force coefficient of 1.932.

B.3 1D Beam Model Using RFEM

In order to compare the results of the numerical solution and calculation according to Eurocode, a 1D beam element model has been created using RFEM. The considered section of the beam element is shown in Figure **2.1** and it is fixed at one end. This beam is subjected to its self-weight and line load. The line load (LL) has been calculated as follow:

$$LL = c_f \cdot q_p(z) \cdot Section\ Width \tag{B.6}$$

The resulted line load is $0.0541\, kN/m^2$. Subjecting the beam element to the aforementioned loads resulted in maximum deflection of $27.7\, mm$ and maximum Von Mises stress of $101.58\, N/mm^2$ (see Figures **B.6** and **B.7**).

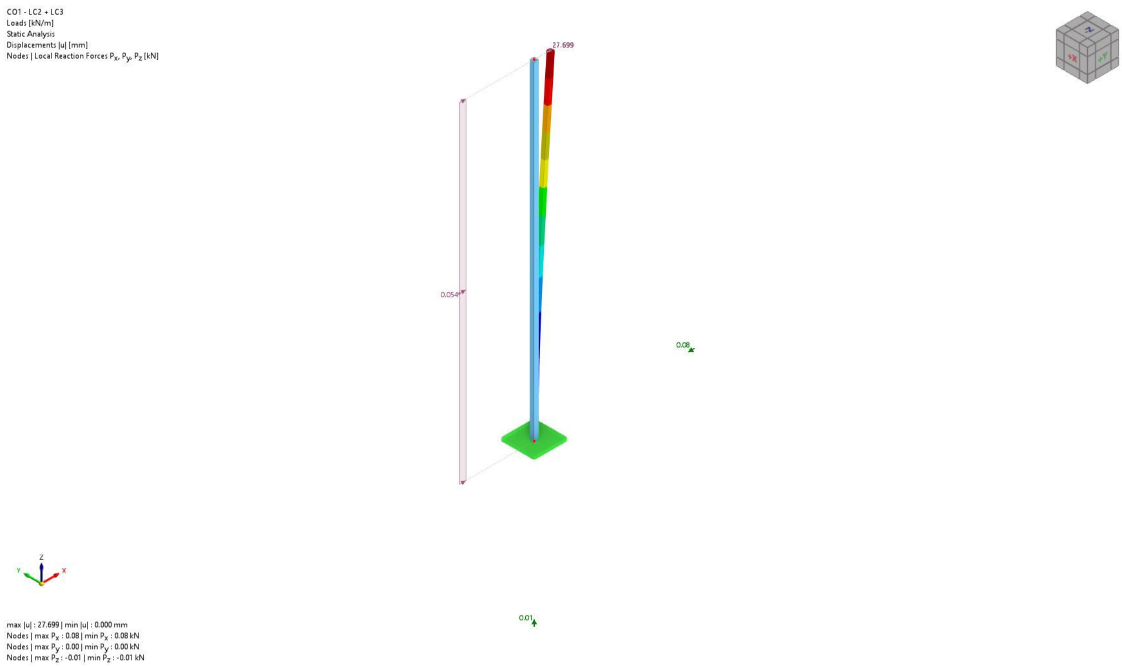

Figure B.6: Maximum Deflection - Beam Model

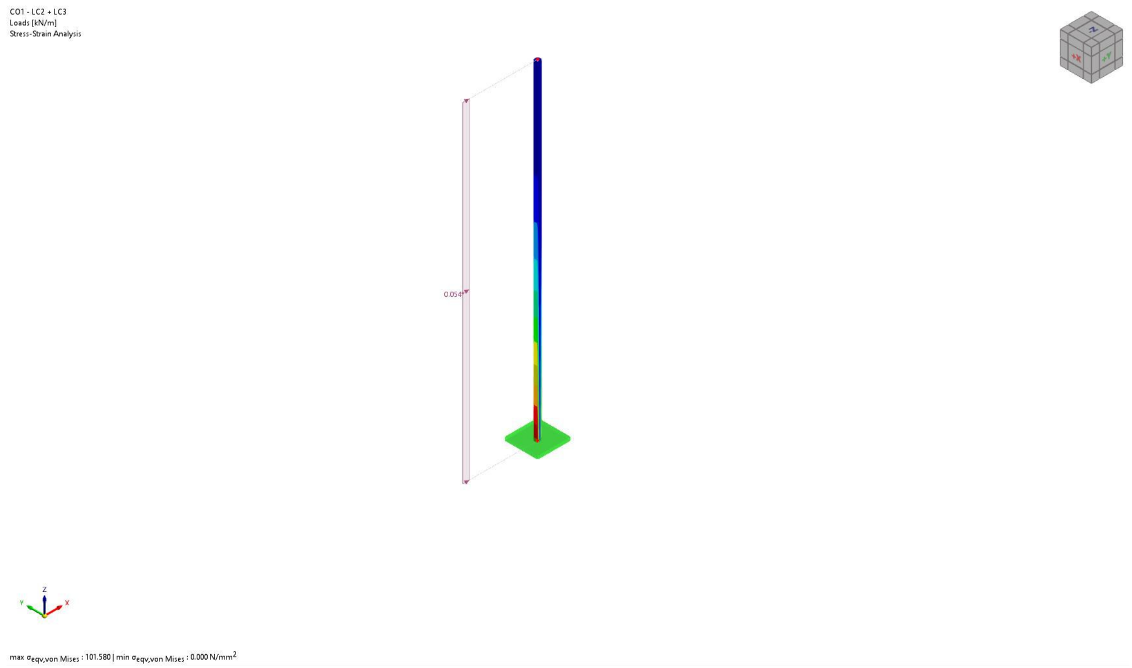

Figure B.7: Maximum Von Mises Stress - Beam Model